NATIONAL ADVISORY COMMITTEE FOR AERONAUTICS

TECHNICAL NOTE 3573

EFFECT OF EXHAUST-NOZZLE EJECTORS ON TURBOJET NOISE GENERATION

By Warren J. North and Willard D. Coles

Lewis Flight Propulsion Laboratory
Cleveland, Ohio

Washington

October 1955

NATIONAL ADVISORY COMMITTEE FOR AERONAUTICS

TECHNICAL NOTE 3573

EFFECT OF EXHAUST-NOZZLE EJECTORS ON TURBOJET NOISE GENERATION

By Warren J. North and Willard D. Coles

SUMMARY

Engine noise levels and jet-velocity profiles have been obtained with several turbojet exhaust-nozzle ejectors. An insignificant reduction in total sound power was realized. At subsonic nozzle pressure ratios, total sound power from exhaust-nozzle ejectors or bypass exit configurations can be calculated from primary-jet parameters only.

INTRODUCTION

Acoustic tests of several turbojet engines and air jets have shown that the total sound power emitted by a jet is nearly proportional to the eighth power of the jet velocity. Theoretical work of reference 1 indicates that jet noise should also depend upon the shear at the jet boundary. It is expected that near the nozzle lip the sound generated by the high-frequency eddy motion is responsible for the high-frequency components of jet noise. At subsonic pressure ratios the bulk of the low-frequency noise can probably be attributed to the large turbulent eddying motion several diameters downstream of the jet exit (ref. 2).

In an effort to reduce noise without reducing the core velocity of the jet, model jet tests were conducted to determine the effect of reduced shear at the jet boundary (ref. 3). Reduced velocity gradients were obtained by adding a constant-diameter extension to the nozzle which resulted in "pipe-flow" velocity profiles. At subsonic pressure ratios the resultant sound levels measured at 30° and 90° to the jet axis were slightly lower than the sound levels measured from a jet with a flat velocity profile. This slight noise reduction (2.5 and 0.5 db at 30° and 90°, respectively) was apparent in spite of an increased jet diameter necessary for equivalent thrust.

The ejector is another device which will modify the velocity profile of a jet. In most jet aircraft an engine exhaust-nozzle ejector is used for cooling purposes. It was desirable, therefore, to investigate the effect of ejectors on jet noise. This report gives the results of such an investigation with a turbojet engine.

APPARATUS AND PROCEDURE

The engine used in these tests was an axial-flow turbojet with an over-all pressure ratio of 1.75 and a sea-level rated thrust of 5000 pounds. The engine was mounted 6 feet above grade level in a free-field thrust stand (fig. 1), that is, with no sound reflecting surfaces near the jet. The cylindrical exit ejectors incorporated ejector to primary-nozzle diameter ratios of 1.2 and 1.4 (fig. 2). Eight spacing ratios of ejector length to primary-nozzle diameter were tested at each of the diameter ratios. The spacing ratios ranged from 0.15 to 1.50. 3850

Engine instrumentation was routed to a control room located 100 feet from the thrust stand at the 240° azimuth, as shown in figure 3. Engine thrust was measured by a strain-gage and potentiometer system. Engine and ejector air flows were determined from ambient temperature and pressure survey rakes at the engine inlet and ejector annulus. Gas temperatures at the ejector exit and at the turbine outlet were recorded on a flight recorder.

Since the nozzle pressure ratios were subsonic, the ejector-exit static pressure was assumed equal to ambient static pressure for all jet Mach number calculations.

Measurements of sound pressure levels were made at 15° intervals in a 270° sector around the engine, as shown in figure 3. No sound pressure measurements were taken in the forward 90° quadrant where the control room was located. For purposes of total sound power calculation, the sound pressures in the two forward 90° quadrants were assumed to be symmetrical. The sound pressure levels were observed on a General Radio Company Type 1551-A Sound-Level Meter 200 feet from the jet nozzle. The frequency distribution of sound pressure was measured at stations 30°, 90°, 135°, and 180° from the jet axis at a distance of 200 feet from the nozzle. The data were taken with a Brüel and Kjaer Audio Frequency Spectrum Recorder type 2311. The frequency range for this instrument is from 35 to 18,000 cps and is divided into 27 one-third octaves. The spectrum recorder was transported in an acoustically insulated panel truck. Prior to each run, the General Radio and Brüel and Kjaer meter-microphone circuits were calibrated with a General Radio Company Type 1552-A Sound-Level Calibrator and General Radio Company Type 1307-A Transistor Oscillator.

The decibel unit is used herein to represent sound pressure level, spectrum level, and total sound power level. Complete definitions and formulas for these acoustic terms are presented in reference 4. Sound pressure level, based on a reference of 0.0002 dyne per square centimeter, is indicated by the General Radio Sound-Level Meter, which responds simultaneously to all frequencies from 20 to 10,000 cps. Spectrum level is the sound pressure level in a finite band width (1/3 octave) corrected to a unit frequency basis. Total sound power level involves a hemispherical integration (ref. 4) of sound pressure and represents all the sound power issuing from a sound source. Sound power level is based on a reference of 10^{-13} watts.

RESULTS AND DISCUSSION

Ejector Performance

Variation in jet-boundary velocity profiles at the ejector exit was obtained by varying the ejector length for a given diameter ratio. Since the variation of over-all net thrust was insignificant, the momentum increase of the induced secondary air was nearly equivalent to the loss in momentum of the primary jet. As shown in figure 4, ejector pumping rates increased as length was increased; however, at a diameter ratio of 1.2 it appears that the peak in the mass-flow-ratio curve will occur at the 1.5 spacing ratio. Mass-flow ratio is defined as the ratio of secondary flow to primary-jet flow. At the maximum ejector length, mass-flow ratios for the 1.2- and 1.4-diameter-ratio ejectors were 23 and 39 percent, respectively.

The ejector-exit velocity profiles at rated engine speed for the 1.2- and 1.4-diameter-ratio ejectors are shown in figures 5(a) and (b), respectively. In order to investigate the primary-jet boundary in more detail, a closely spaced total-pressure rake was installed; and the resultant Mach number profiles are shown in figure 6. The Mach number profiles are shown for three values of engine speed. Near the jet boundary the velocity and Mach number gradients decreased with increasing ejector diameter ratio and spacing ratio. The jet velocity continually decreased radially outward from the main body of the jet. Since a temperature gradient also occurs near the jet boundary, the Mach number profiles show a peak near the boundary for the smaller ejector spacing ratios.

Ejector Sound Pressure Measurements

Typical polar plots of sound pressure level are shown in figure 7 for the two diameter-ratio ejectors at various spacing ratios. The sound field for the standard engine is also shown. At a given azimuth only slight variations are noted among the ejector and standard-engine sound levels. With one exception all the ejectors caused a slight decrease in maximum sound pressure level, which occurred at the 30° azimuth. The exception was an ejector (fig. 7(b)) with a spacing ratio of 0.90 that created acoustic resonance and thereby produced higher sound pressure levels over the entire field.

In order to obtain an insight as to the causes of these sound pressure variations, the spectrum levels were examined (figs. 8 and 9). The spectrum data are presented for rated engine speed at azimuth angles of 30°, 90°, and 135° and at an observer distance of 200 feet. In the case of the 1.2-diameter-ratio ejector (fig. 8(a)), it can be seen that at the 30° azimuth there is a general decrease in spectrum level for frequencies between 230 and 370 and also for frequencies above 1000 cycles. The high-frequency attenuation is apparent to a lesser extent with the 1.4-diameter-ratio ejector, as shown in figure 9(a). At the 90° and 135° azimuth angles (figs. 8(b) and (c) and 9(b) and (c)) this high-frequency attenuation is not apparent. The previously mentioned resonance associated with the 0.9-spacing-ratio ejector is seen as a discrete 160-cycle frequency at the 30° azimuth in figure 9(a). At 90° and 135° (figs. 9(b) and (c), respectively) this resonance also includes the 125-cycle band. The high-frequency attenuation is most pronounced with the longest ejectors, but the low-frequency noise was in general unaffected by any of the ejector configurations. 3850

The spectral distribution of sound intensity at the 30° azimuth for the standard engine is shown in figure 10. The ordinate of the figure is cumulative sound intensity. The nearly vertical portions of the curve indicate frequency bands with large noise content. For the frequency ranges wherein the ejectors cause noise attenuation (230 to 370 and above 1000 cps), only 10 percent of the total sound intensity is involved. Since 10 percent of the sound intensity corresponds to only 1/2 decibel, little sound reduction is possible by reducing the sound intensity in those frequency ranges. This ineffectiveness of the ejectors as noise suppressors is also noted in figure 7, which shows insignificant attenuation at the 30° azimuth.

Although decreased velocity gradients at the ejector exits were noted as ejector length increased, it must be remembered that a region of intense shear existed inside the ejector shroud near the primary-jet nozzle. The intensity of this internal shear region was reduced, however, as the pumping rate or mass-flow ratio increased. It would be expected that the previously mentioned high-frequency attenuation could be partially attributed to the reduced velocity gradients both within the ejector and at the ejector exit. Some attenuation may be due to reflection of the high-frequency pressure waves within the ejector shroud and also to the passage of these waves downstream through the diverging primary jet.

Total Sound Power Levels

In figure 11 is presented the total sound power levels in terms of watts and decibels for the ejectors as well as for several familiar engine sound power levels which are included for comparison purposes. The afterburner level was determined from the data in reference 5. All the sound power data for the various exit configurations were obtained with the same engine.

Transition from rated engine operation to maximum-thrust afterburner operation resulted in an increase from 168 to 177 decibels. Throttling from rated engine speed to 80 percent rated speed resulted in an 11-decibel decrease. In contrast with these significant sound power variations, all the ejector sound power levels, with one exception, range between zero and 2 decibels below the standard engine levels. Although the longer ejectors caused greater high-frequency sound attenuation, there was only a slight downward trend in the total power level as spacing ratio was increased. These results were expected since the sound power involved in the high-frequency range is but a small part of the power in the over-all spectrum.

The theoretical work in reference 1 indicates that for subsonic pressure ratios the total sound power should be proportional to the Lighthill parameter

$$\frac{\rho_0 A V^8}{a_0^5}$$

where

ρ_0 ambient air density

A nozzle-exit area

V jet velocity

a_0 ambient acoustic velocity

In figure 12 the total sound power levels from figure 11 are plotted against this Lighthill parameter. The curve was drawn through the data points obtained with the standard nozzles. When the parameter values for the ejectors were computed, the governing factor, jet velocity, was calculated from measured thrust and primary mass flow. It can be seen that all the sound power data fall within 2 decibels of the standard-engine curve. In contrast, when the parameter was computed on the basis of the ejector-exit area and total mass flow, a maximum deviation of 6 decibels was apparent. It is evident, therefore, that the sound power generated by an exhaust-nozzle ejector can be predicted from the characteristics of the primary jet.

CONCLUDING REMARKS

In order to determine the acoustic effects of jet-exit ejectors, an experimental program was conducted and the following conclusions are presented:

1. No significant decrease in jet-engine noise associated with the use of ejectors was found when the sound power was evaluated at subsonic nozzle pressure ratios.

2. The ejector shrouds decreased the high-frequency portion of jet noise. Since only a small part of turbojet noise occurs in the high-frequency spectrum, this reduction in high-frequency noise caused little reduction in total sound power.

3. Regardless of the exit configuration, the governing factor in jet-noise generation was the velocity of the primary jet. When total sound power was plotted against the Lighthill parameter for the primary jet, the data for all the exit modifications showed a variation of only 2 decibels from the standard-nozzle curve.

4. Recent unpublished ejector data obtained with a model air jet at a diameter ratio of 1.4 and spacing ratio of 1.5 show significant decreases in total sound power at nozzle pressure ratios in excess of 3.0. Since conventional operation of most jet aircraft does not result in high nozzle pressure ratios at low altitude, the use of ejectors at high pressure ratios is not apt to bring about significant noise reduction as observed from the ground.

5. The presence of the low-velocity outer-annular jet has been considered to be an important factor in the potential noise reduction associated with the bypass engine. Since bypass jet flow can be somewhat simulated by exit ejector flow, it would appear that for moderate bypass mass-flow ratios the primary jet rather than bypass interaction will largely determine the bypass engine noise level. Since the primary jet of a bypass engine operates at a lower velocity than that of an equivalent-thrust turbojet, the bypass engine should produce a lower noise level primarily by virtue of the lower energy level in the primary jet.

Lewis Flight Propulsion Laboratory
National Advisory Committee for Aeronautics
Cleveland, Ohio, August 9, 1955

3850

REFERENCES

1. Lighthill, M. J.: On Sound Generated Aerodynamically. II - Turbulence as a Source of Sound. Proc. Roy. Soc. (London), ser. A, vol. 222, Feb. 23, 1954, pp. 1-32.

2. Lassiter, Leslie W., and Hubbard, Harvey H.: Experimental Studies of Noise from Subsonic Jets in Still Air. NACA TN 2757, 1952.

3. Powell, A.: The Influence of the Exit Velocity Profile on the Noise of a Jet. The Aero. Quart., vol. IV, pt. 4, Feb. 1954, pp. 341-360.

4. Bolt, R. H., Lukasik, S. J., Nolle, A. W., and Frost, A. D., eds.: Handbook of Acoustic Noise Control. Vol. I. Physical Acoustics. WADC Tech. Rep. 52-204, Aero. Medical Lab., Wright Air Dev. Center, Wright-Patterson Air Force Base, Dec. 1952. (Contract No. AF 33(038)-20572, RDO No. 695-63.)

5. North, Warren J., Callaghan, Edmund E., and Lanzo, Chester D.: Investigation of Noise Field and Velocity Profiles of an Afterburning Engine. NACA RM E54G07, 1954.

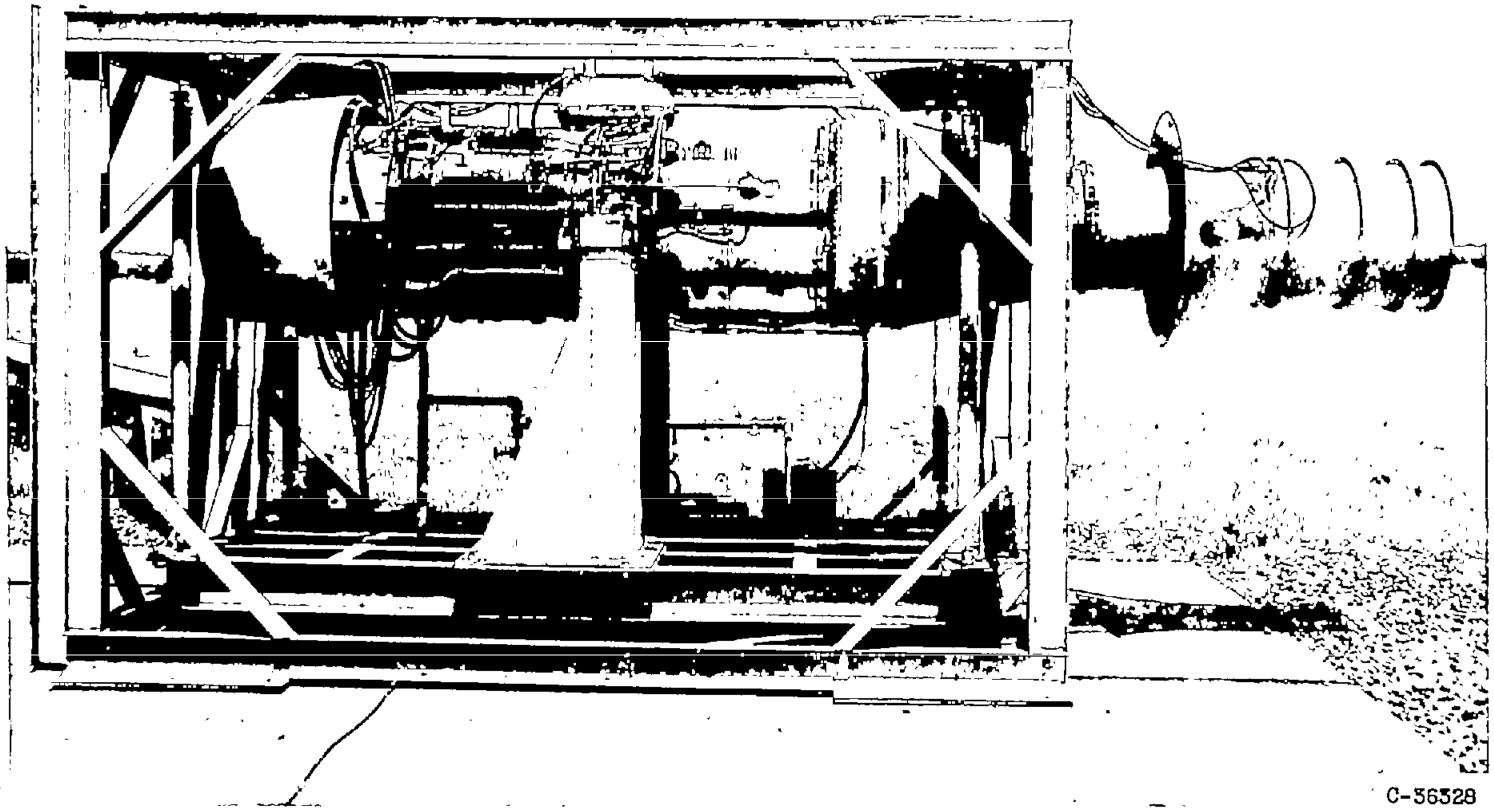

Figure 1. - Thrust stand with ejector installation.

3850
CW-2

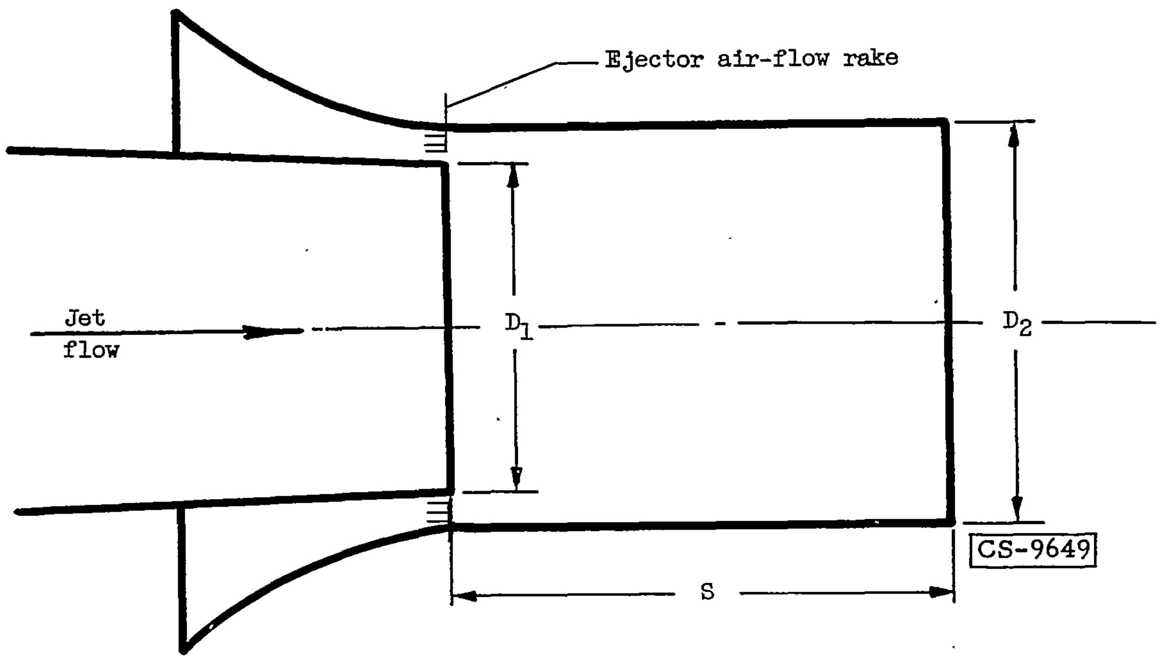

Figure 2. - Ejector configurations. Diameter ratios D_2/D_1, 1.2 and 1.4; spacing ratios, $0.15 < \frac{S}{D_1} < 1.50$.

3850

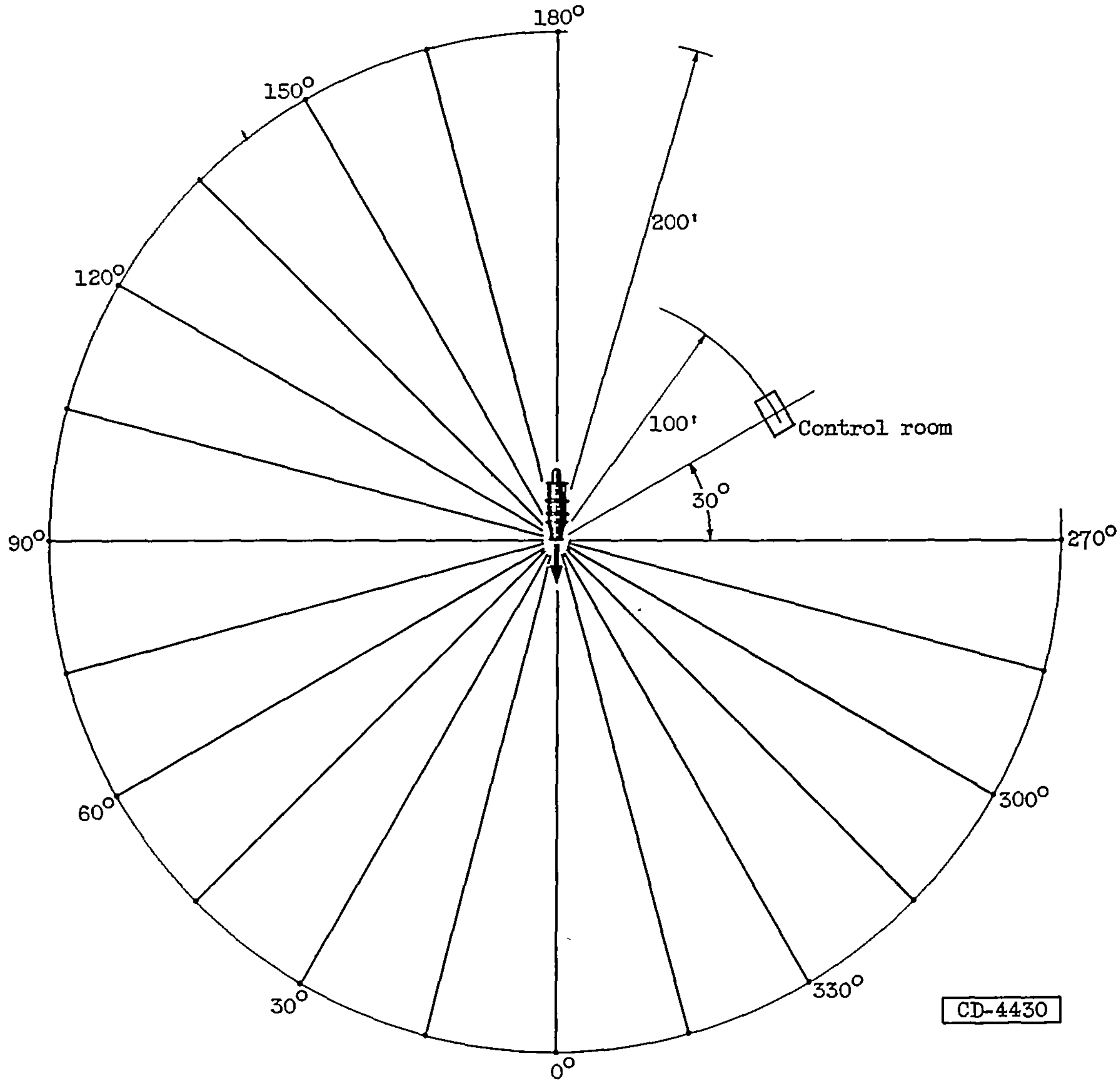

Figure 3. - Location of sound survey stations and control room.

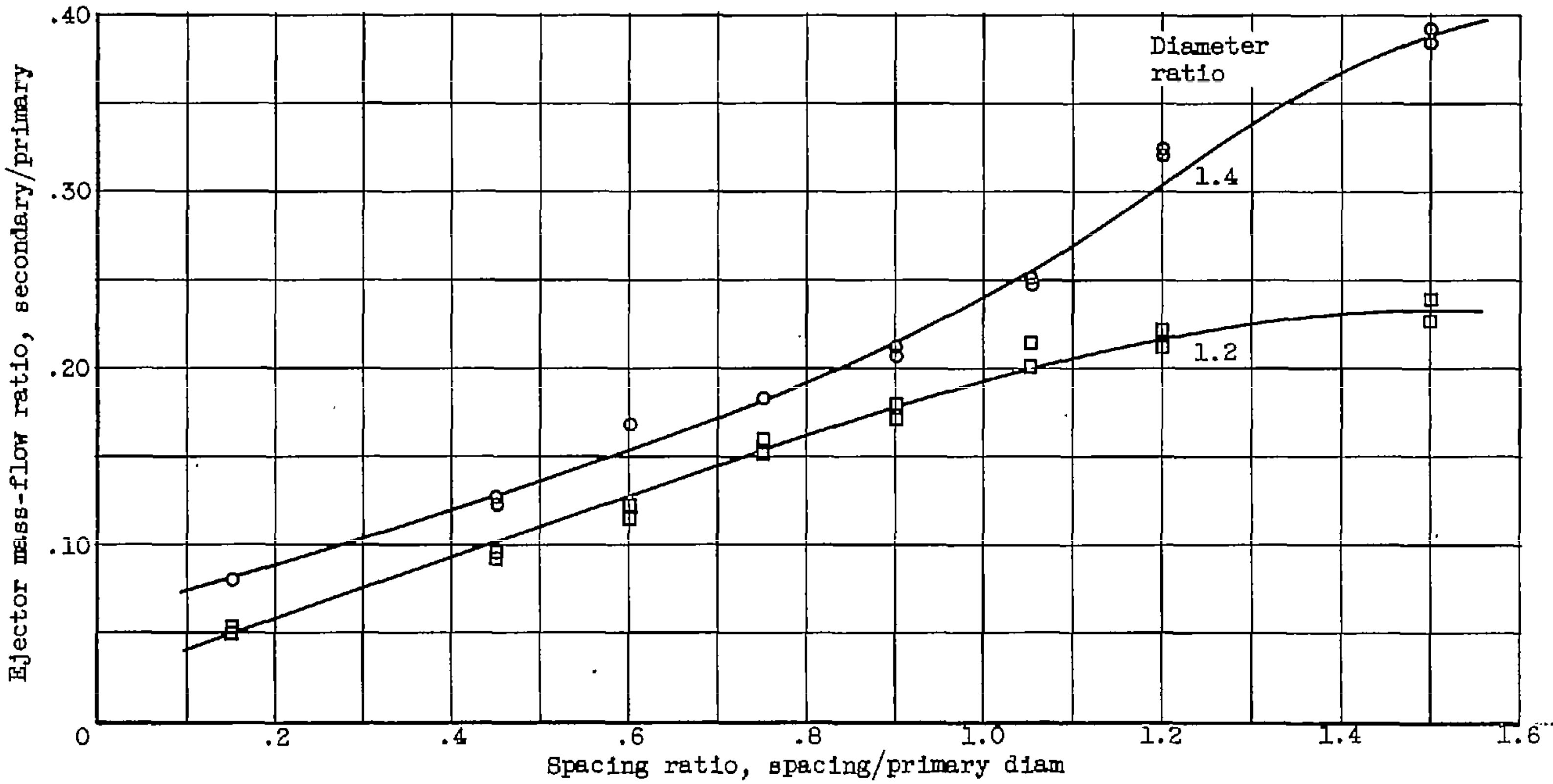

Figure 4. - Variation of ejector mass-flow ratio with spacing ratio. Primary-gas temperature, 1250° F.

3850

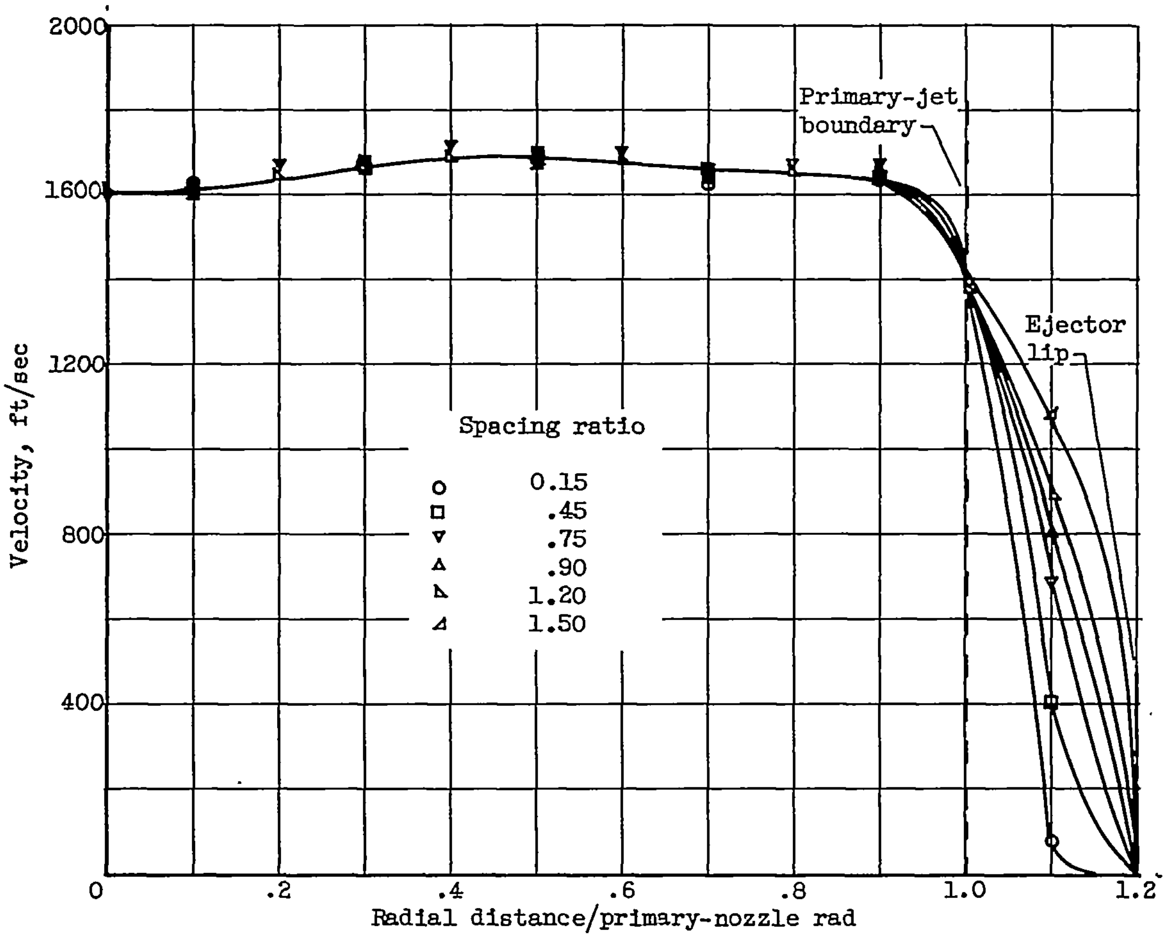

(a) Diameter ratio, 1.2.

Figure 5. - Velocity profiles at ejector exit.

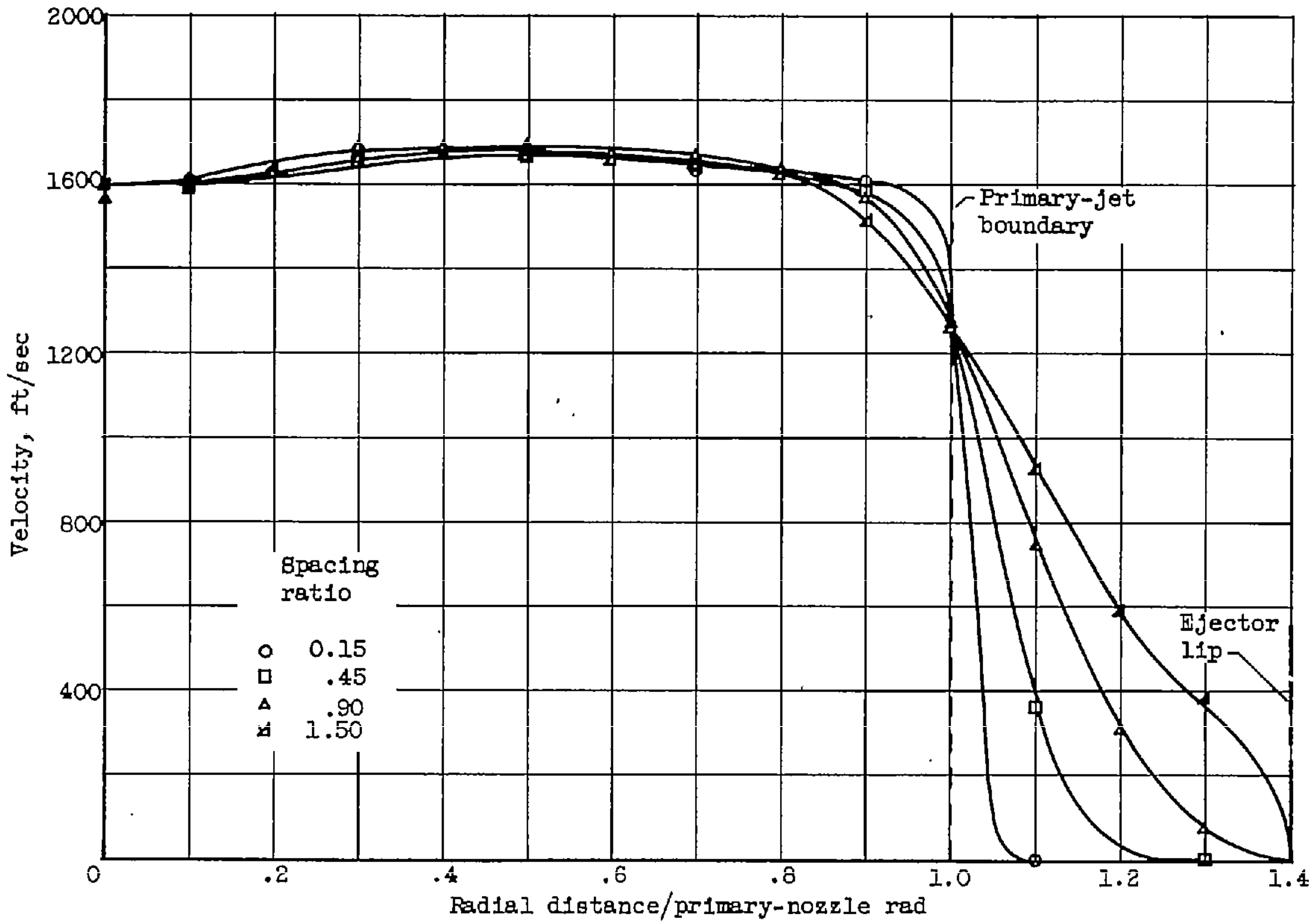

(b) Diameter ratio, 1.4.

Figure 5. - Concluded. Velocity profiles at ejector exit.

3850

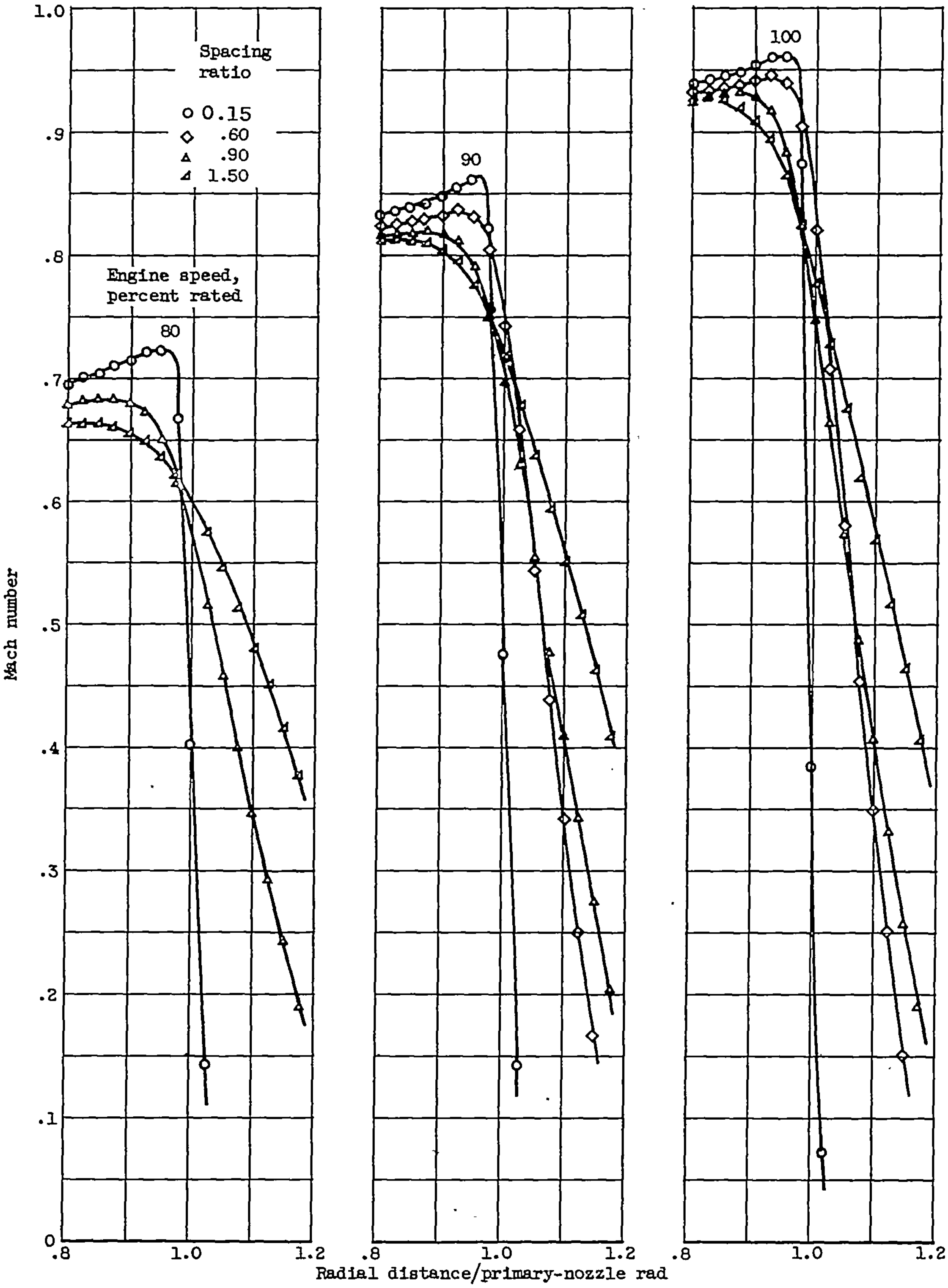

(a) Diameter ratio, 1.2.

Figure 6. - Mach number profiles at ejector exit.

3850

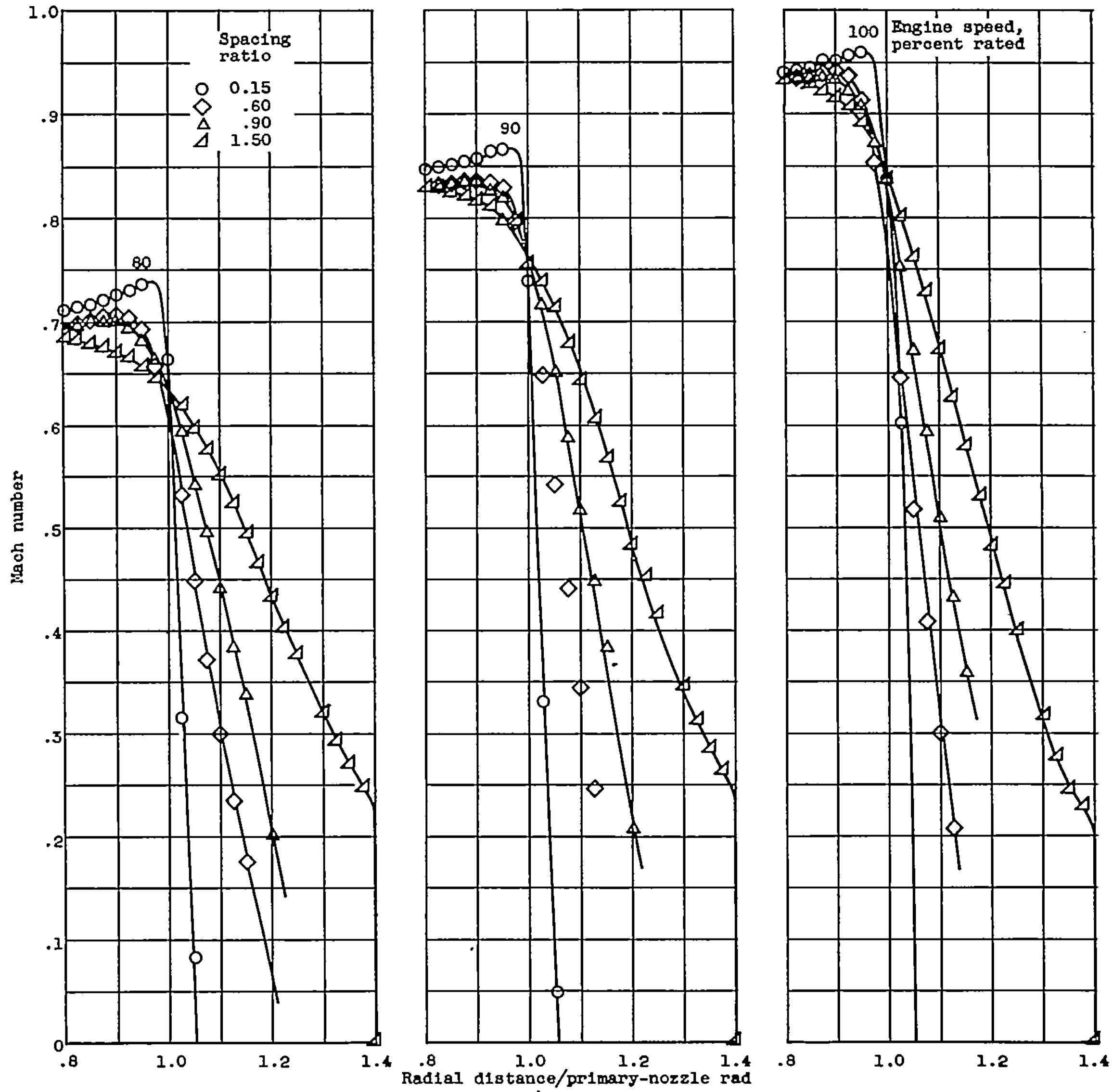

(b) Diameter ratio, 1.4.

Figure 6. - Concluded. Mach number profiles at ejector exit.

3850

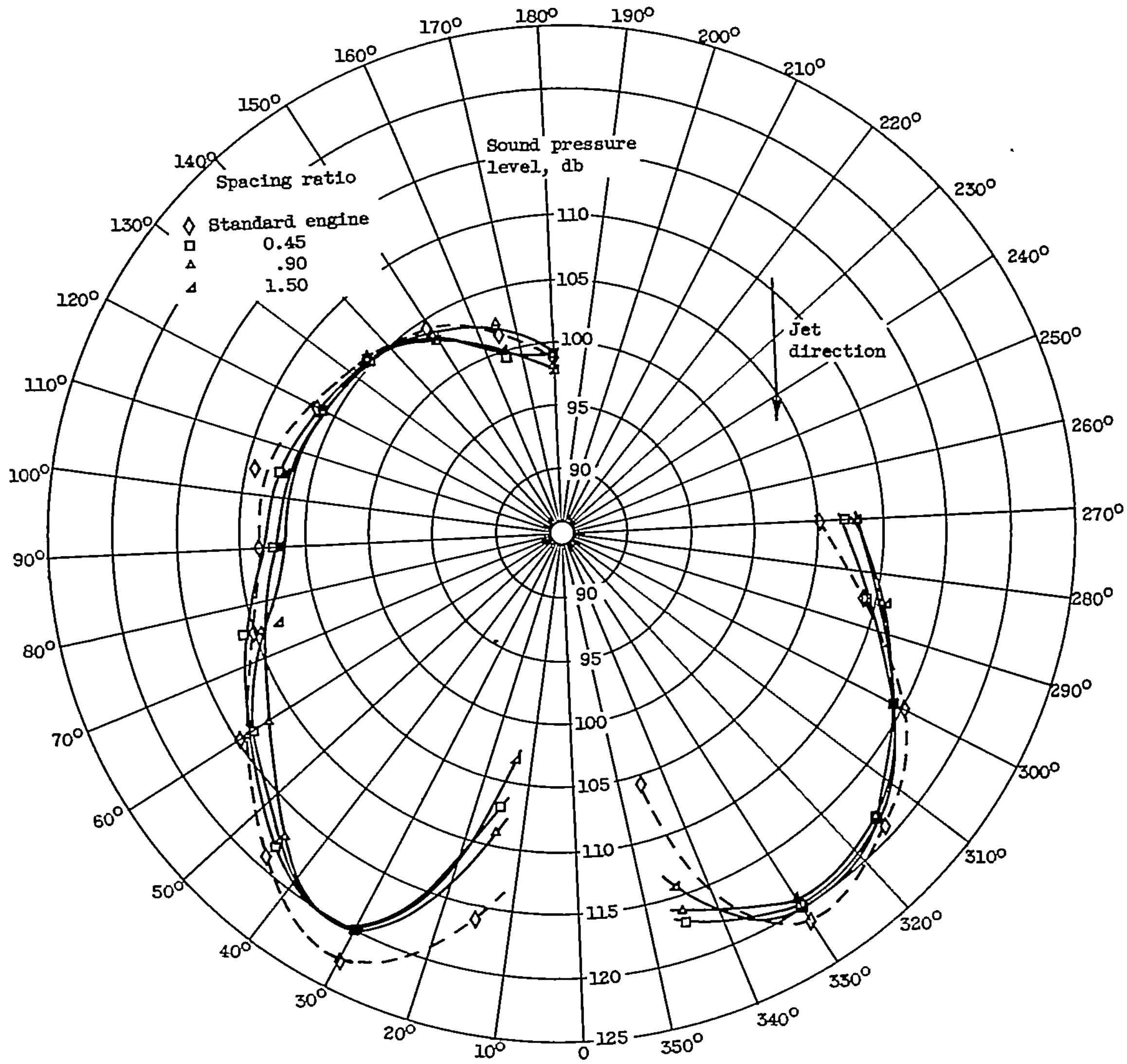

(a) Diameter ratio, 1.2.

Figure 7. - Sound pressure field at distance of 200 feet.

3850

CW-3

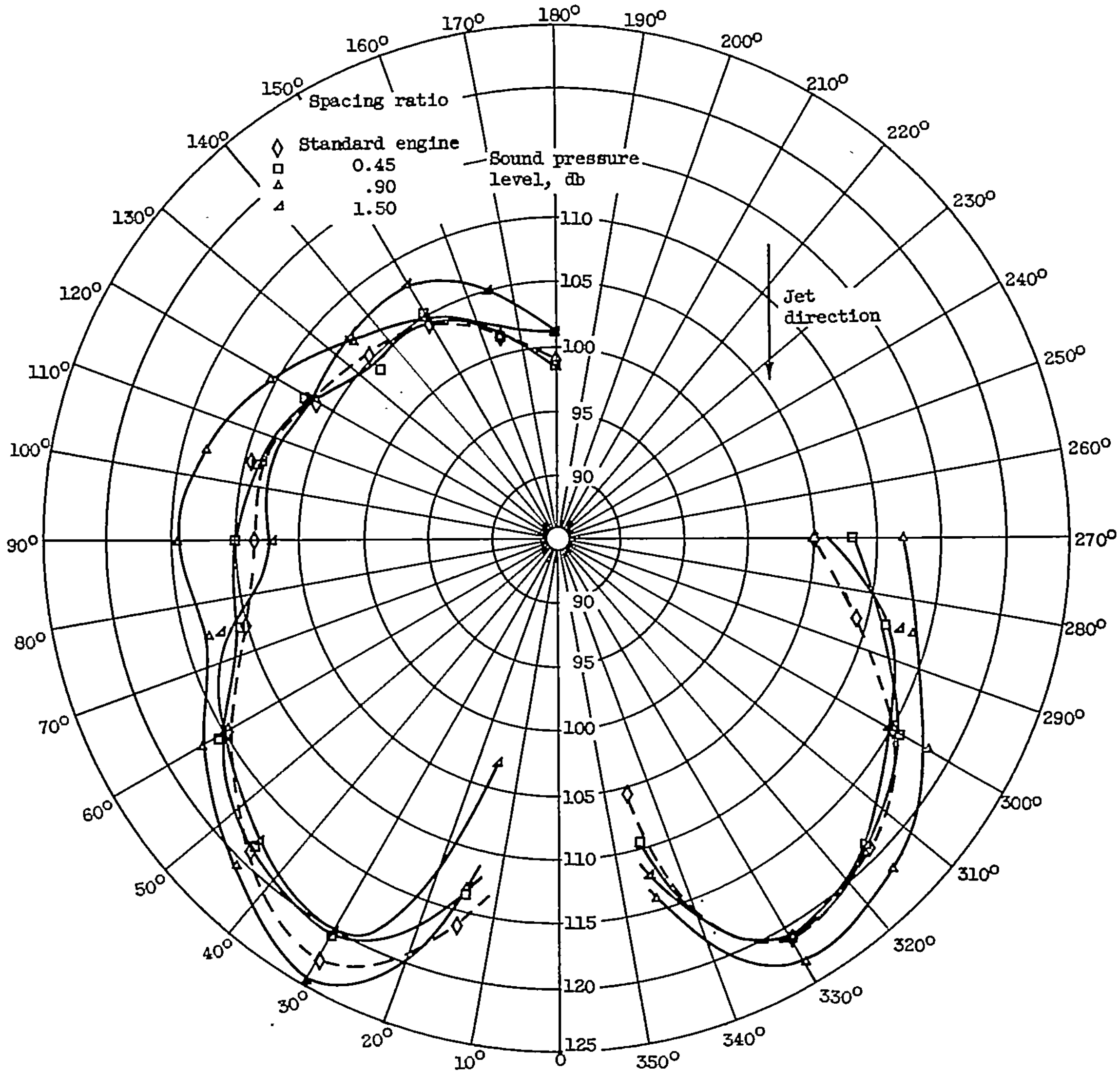

(b) Diameter ratio, 1.4.

Figure 7. - Concluded. Sound pressure field at distance of 200 feet.

3850

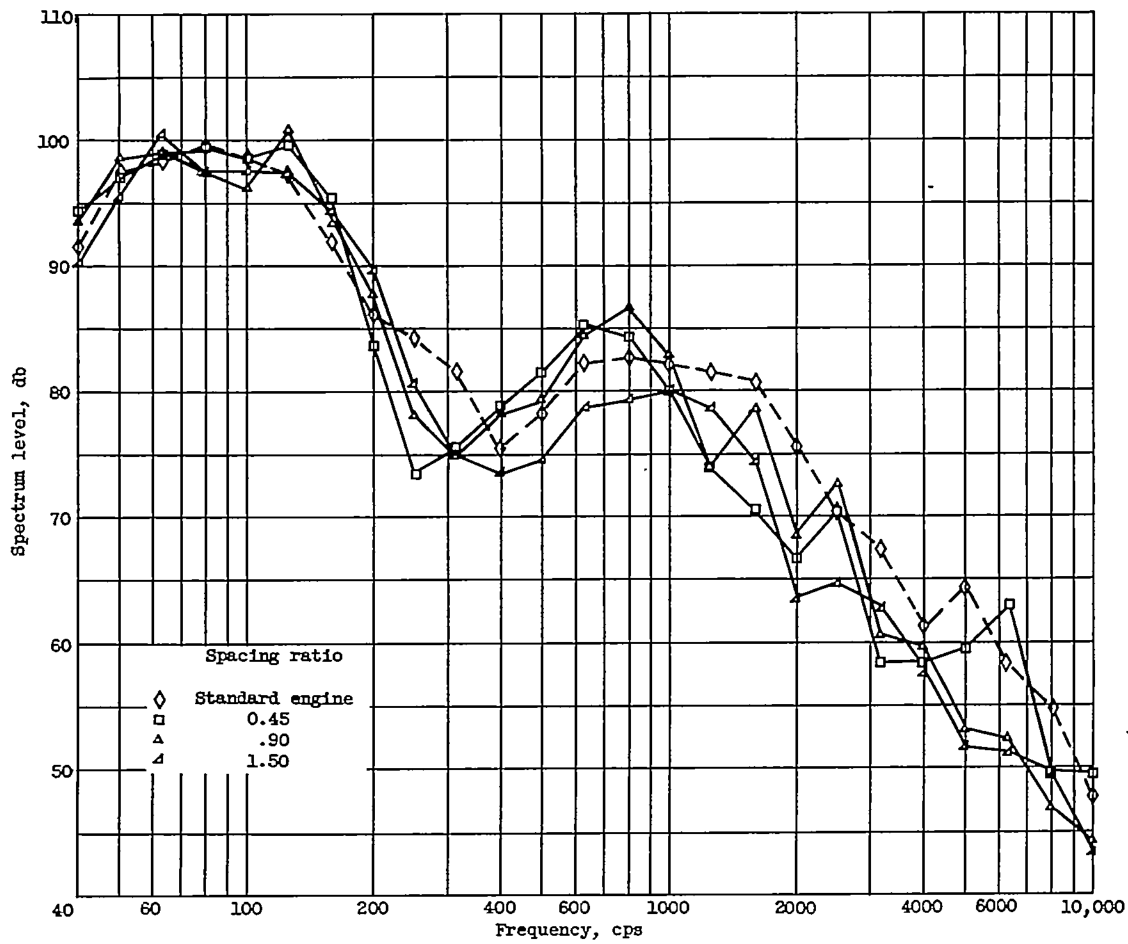

(a) Azimuth angle, 30°.

Figure 8. - Spectrum level at rated engine speed and distance of 200 feet. 1.2-Diameter-ratio ejector.

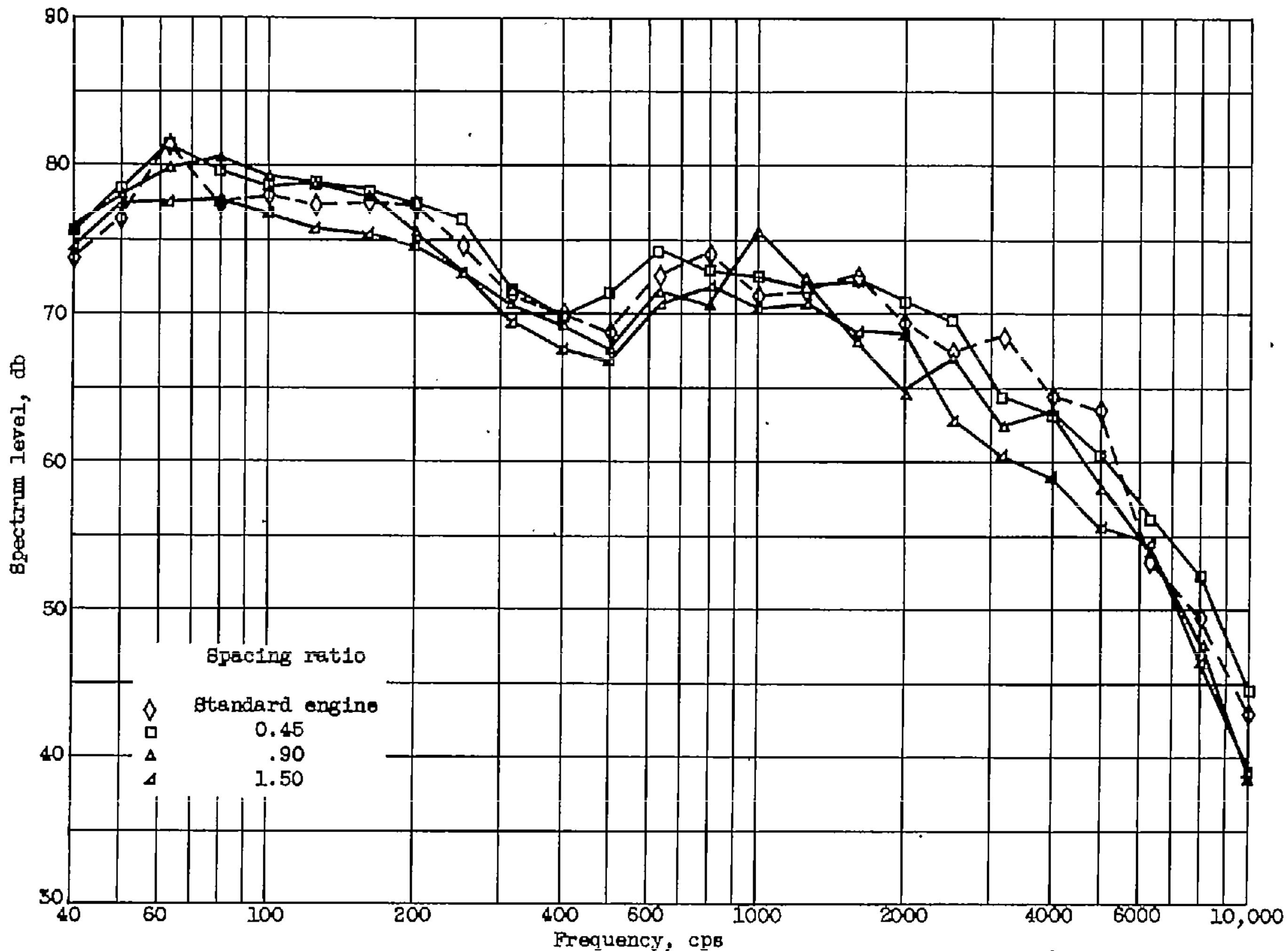

(b) Azimuth angle, 90°.

Figure 8. - Continued. Spectrum level at rated engine speed and distance of 200 feet. 1.2-Diameter-ratio ejector.

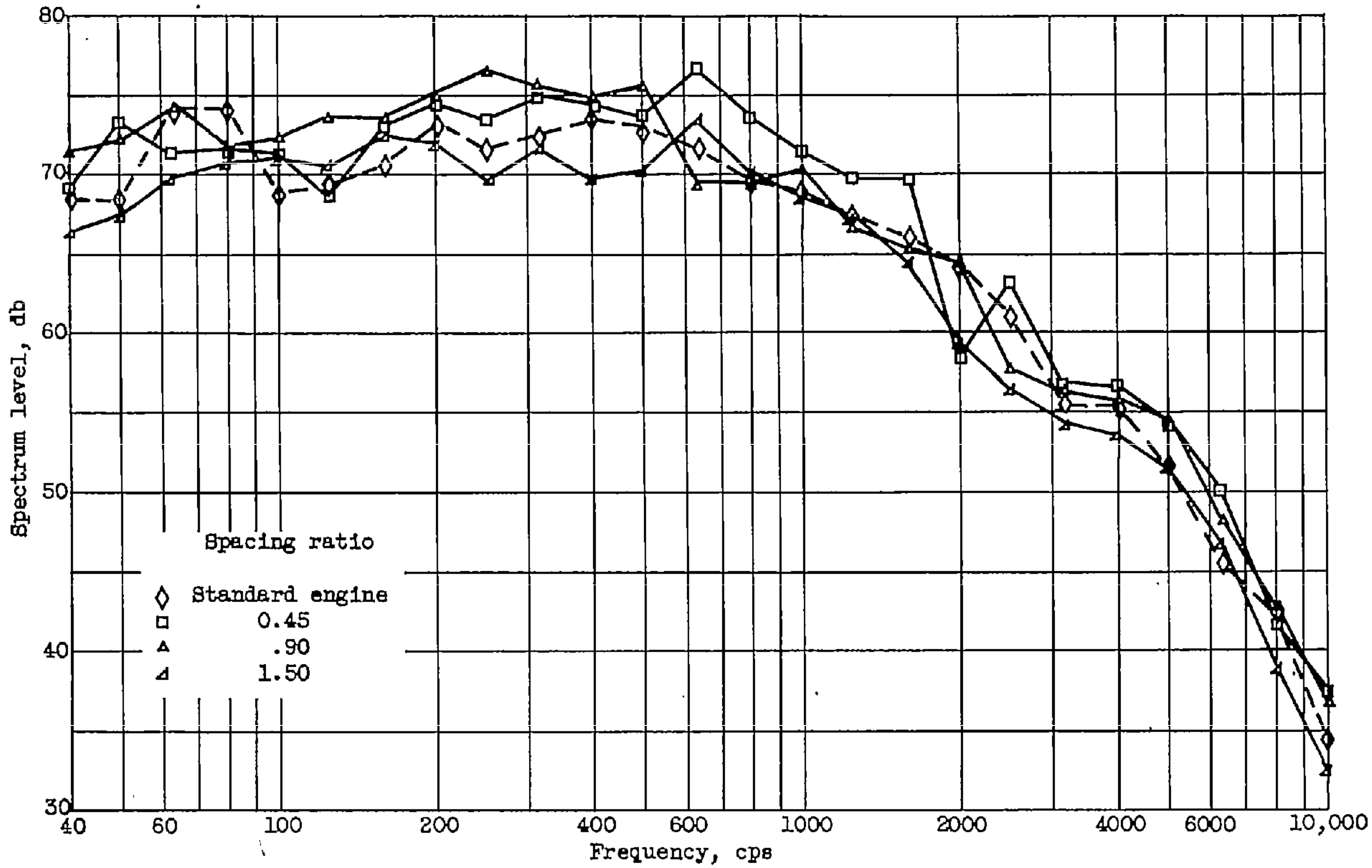

(c) Azimuth angle, 135°.

Figure 8. - Concluded. Spectrum level at rated engine speed and distance of 200 feet. 1.2-Diameter-ratio ejector.

3850

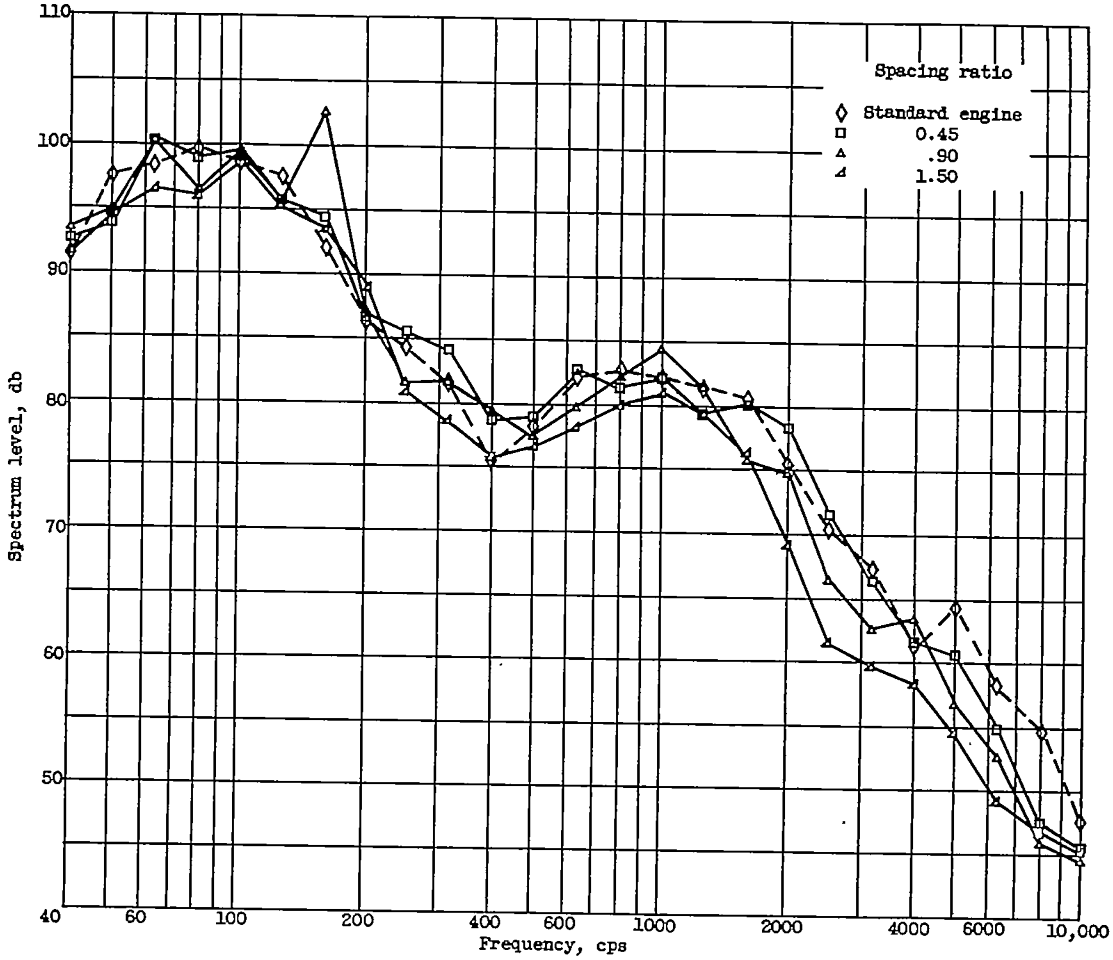

(a) Azimuth angle, 30°.

Figure 9. - Spectrum level at rated engine speed and distance of 200 feet. 1.4-Diameter-ratio ejector.

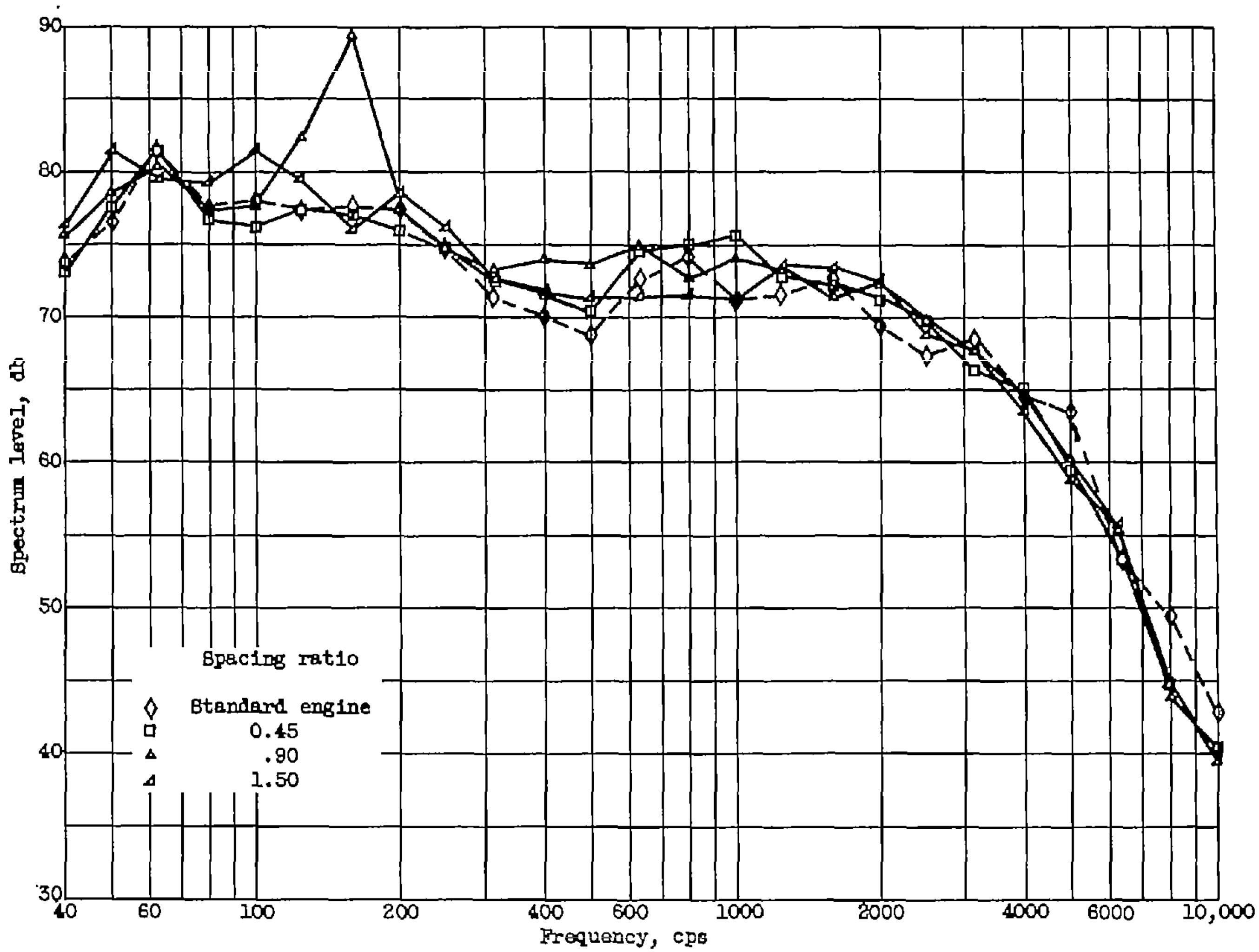

(b) Azimuth angle, 90°.

Figure 9. - Continued. Spectrum level at rated engine speed and distance of 200 feet. 1.4-Diameter-ratio ejector.

3850

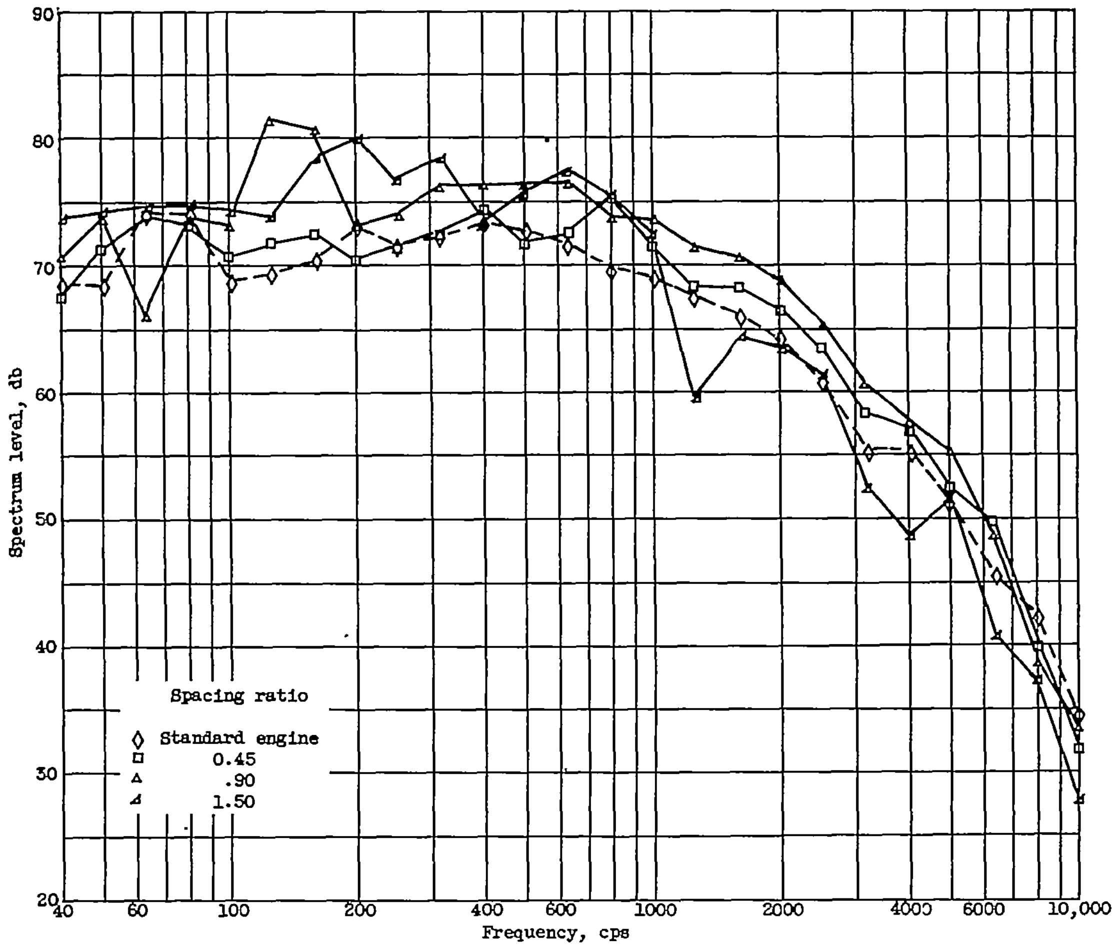

(c) Azimuth angle, 135°.

Figure 9. - Concluded. Spectrum level at rated engine speed and distance of 200 feet. 1.4-Diameter-ratio ejector.

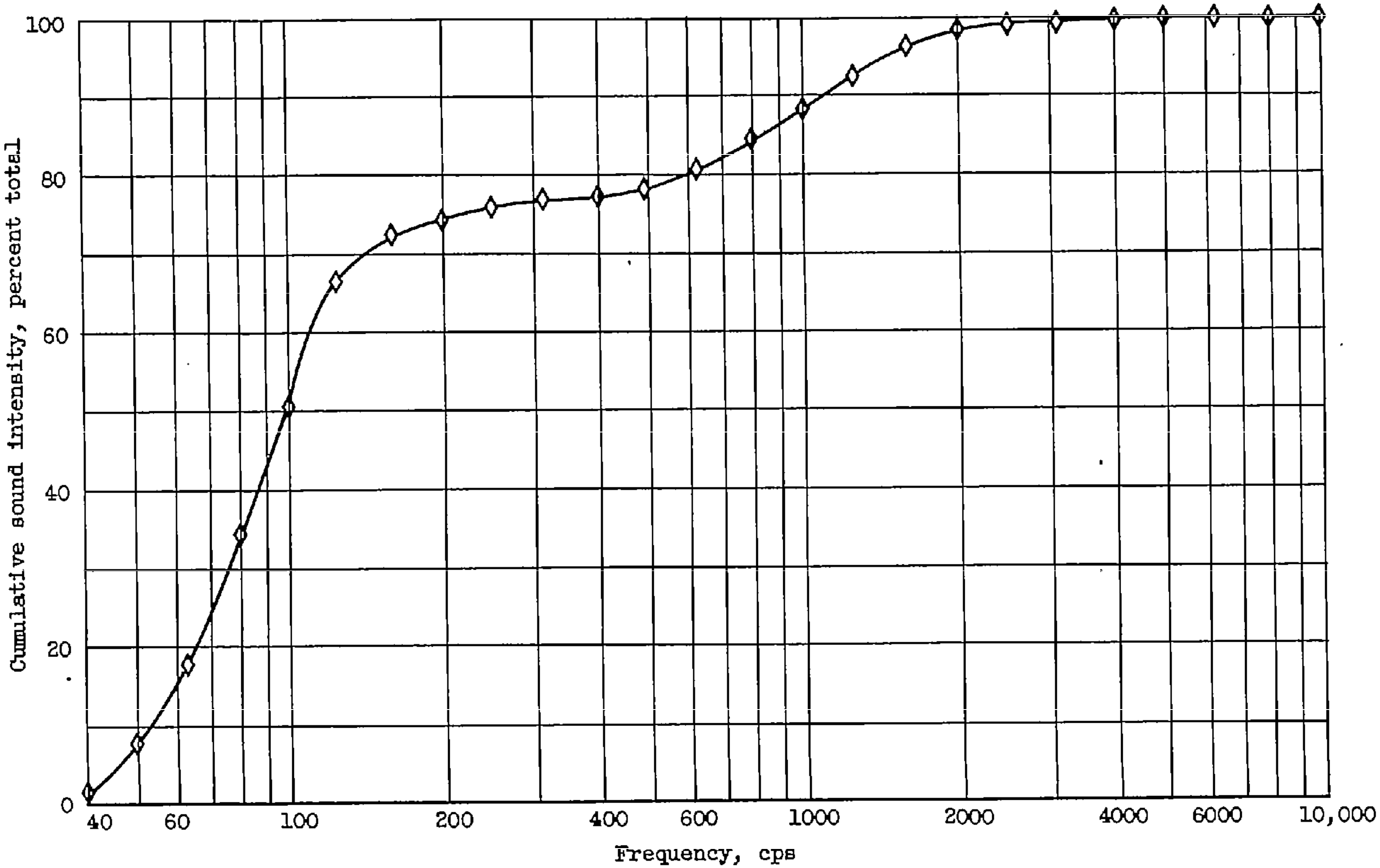

Figure 10. - Spectral distribution of sound intensity for standard engine at 30° azimuth.

3850

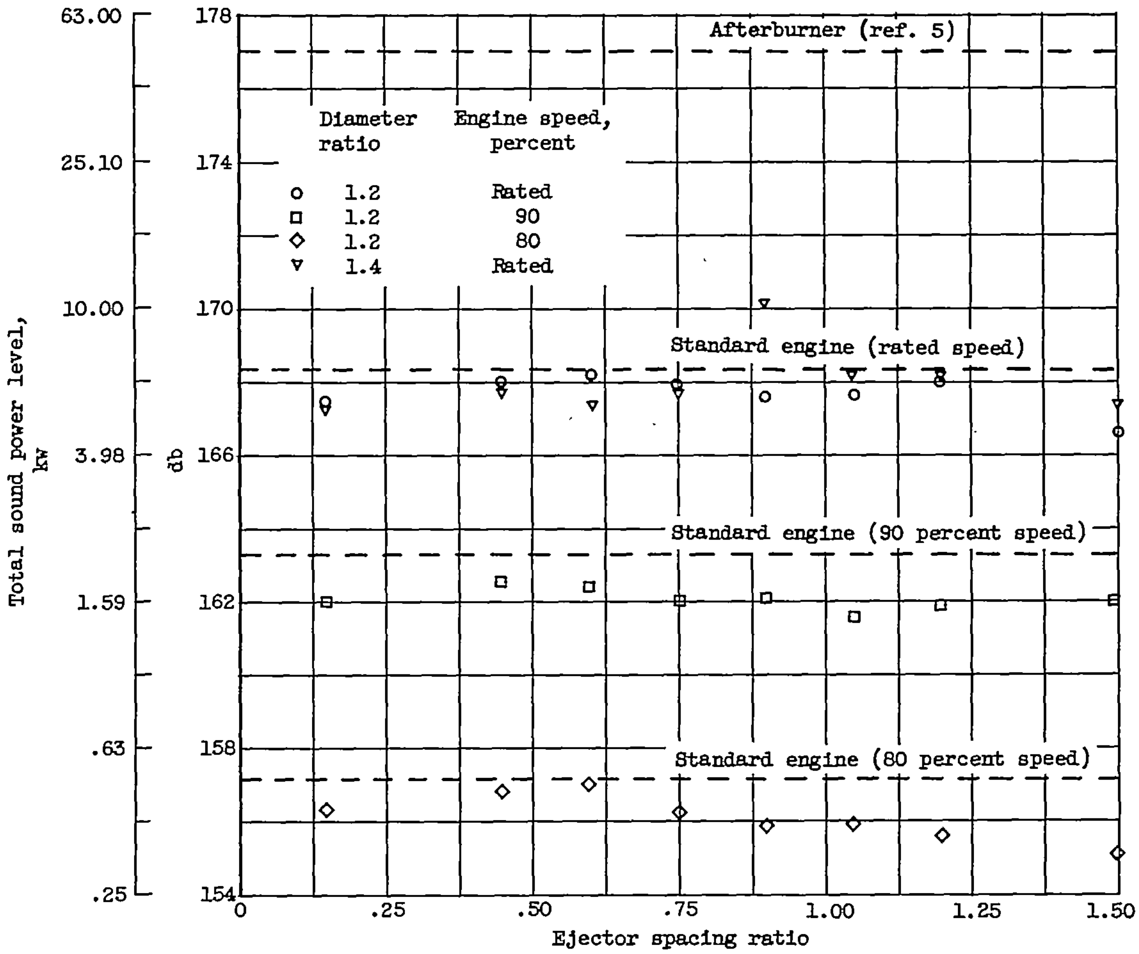

Figure 11. - Comparison of total sound power levels.

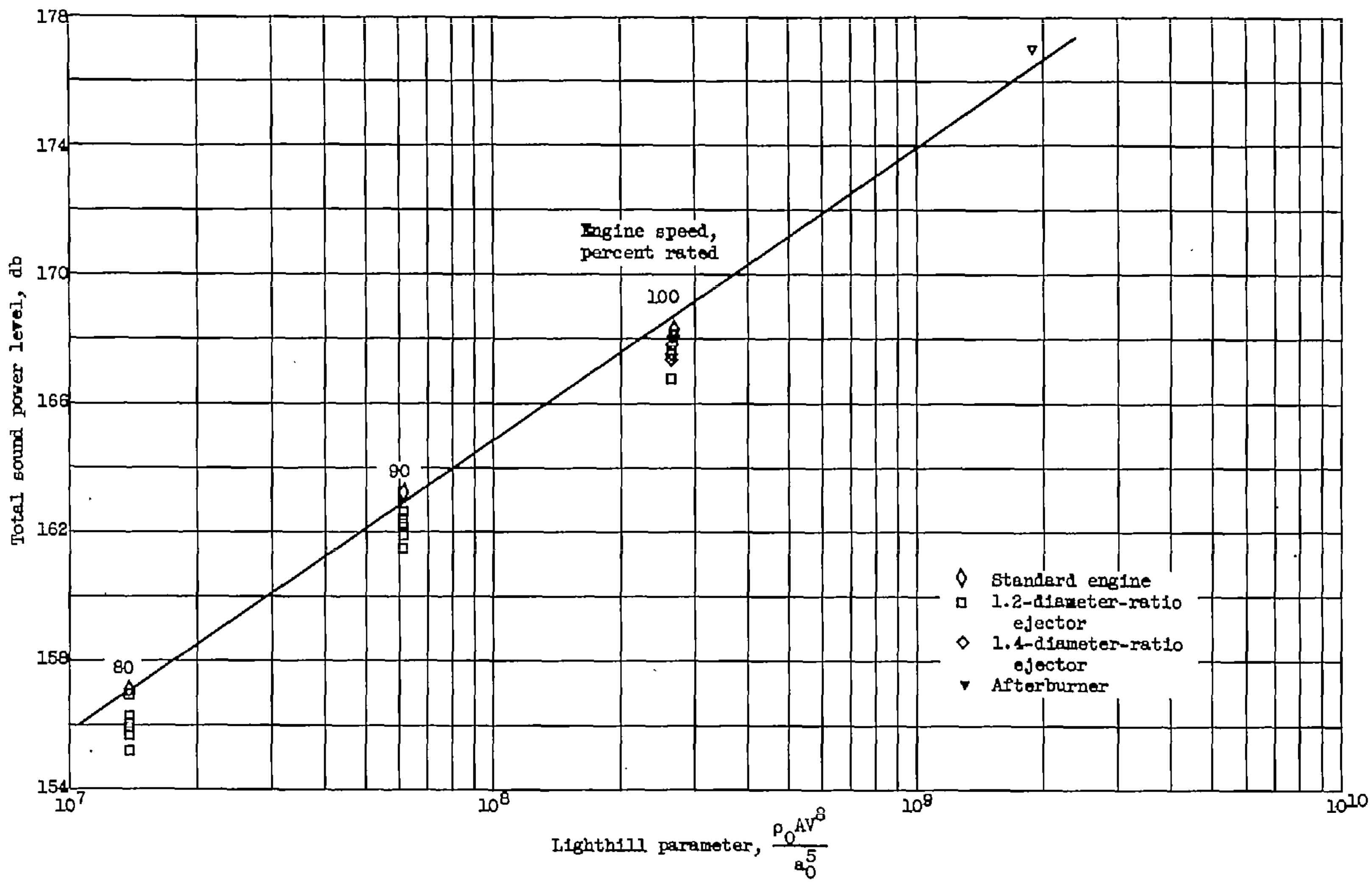

Figure 12. - Variation of total sound power with Lighthill parameter.